REFERENCES

Bardin N, Anfosso F, Massé JM, *et al.* (2001) Identification of CD146 as a component of the endothelial junction involved in the control of cell-cell cohesion. *Blood* 98: 3677–84

Dagur PK, Biancotto A, Wei L, *et al.* (2011) MCAM-expressing CD4(+) T cells in peripheral blood secrete IL-17A and are significantly elevated in inflammatory autoimmune diseases. *J Autoimmun* 37: 319–27

Dagur PK, Tatlici G, Gourley M, *et al.* (2010) CD146+ T lymphocytes are increased in both the peripheral circulation and in the synovial effusions of patients with various musculoskeletal diseases and display pro-inflammatory gene profiles. *Cytometry B Clin Cytom* 78:88–95

Elshal MF, Khan SS, Raghavachari N, *et al.* (2007) A unique population of effector memory lymphocytes identified by CD146 having a distinct immunophenotypic and genomic profile. *BMC Immunol* 8:29

Elshal MF, Khan SS, Takahashi Y *et al.* (2005) CD146 (Mel-CAM), an adhesion marker of endothelial cells, is a novel marker of lymphocyte subset activation in normal peripheral blood. *Blood* 106:2923–4

Guezguez B, Vigneron P, Lamerant N *et al.* (2007) Dual role of melanoma cell adhesion molecule (MCAM)/CD146 in lymphocyte endothelium interaction: MCAM/CD146 promotes rolling via microvilli induction in lymphocyte and is an endothelial adhesion receptor. *J Immunol* 179:6673–85

Kagami S, Rizzo HL, Lee JJ *et al.* (2010) Circulating Th17, Th22, and Th1 cells are increased in psoriasis. *J Invest Dermatol* 130:1373–83

Larochelle C, Cayrol R, Kebir H *et al.* (2012) Melanoma cell adhesion molecule identifies encephalitogenic T lymphocytes and promotes their recruitment to the central nervous system. *Brain* 135(Part 10):2906–24

Mehta NN, Yu Y, Saboury B *et al.* (2011) Systemic and vascular inflammation in patients with moderate to severe psoriasis as measured by [18F]-fluorodeoxyglucose positron emission tomography-computed tomography (FDG-PET/CT): a pilot study. *Arch Dermatol* 147:1031–9

JIDOpen

A Rac1-Independent Role for P-Rex1 in Melanoblasts

Journal of Investigative Dermatology (2015) **135,** 314–318; doi:10.1038/jid.2014.323; published online 11 September 2014

TO THE EDITOR

Given the recent discovery of *RAC1*-activating mutations in melanoma, and our finding that PIP_3-dependent Rac-exchanger 1 (*PREX1*) is overexpressed and drives metastasis in this cancer, an important question is to establish whether the functions of P-Rex1 are mediated specifically by Rac alone (Lindsay *et al.*, 2011; Berger *et al.*, 2012). Here we describe a Rac1-independent *in vivo* role for P-Rex1 through identification and characterization of a mouse coat color phenotype. P-Rex1 is a guanine-nucleotide exchange factor (GEF) for Rac, whose primary cell function is induction of actin-mediated membrane ruffling and lamellipodia formation at the leading edge of cell migration (Welch *et al.*, 2002; Hill *et al.*, 2005; Barber *et al.*, 2007).

To investigate this question we decided to examine the role of Rac1 and P-Rex1 in melanoblast development. Previously, we reported a ''white belly'' phenotype of mice with *Prex1* deletion (Lindsay *et al.*, 2011). Impaired melanoblast migration was mostly responsible for this phenotype, with melanoblasts lacking at the most distal points of migration (belly and paws). Constitutive deletion of *Rac1* is embryonically lethal, but a coat color defect of mice with melanocyte-specific *RAC1* abrogation (*Tyr::Cre* $Rac1^{fl/fl}$) has also been described; these mice have a larger belly spot on their ventral side, suggesting that alternative Rho-GTPases can be activated to enable melanoblast migration to the perimeter of the *Tyr::Cre* $Rac^{fl/fl}$ white belly (Sugihara *et al.*, 1998; Li *et al.*, 2011). A role for Rac1 in proliferation was also observed, as there was a marked reduction of melanoblast numbers in this phenotype. In line with these previous studies, and because mice with melanocyte-specific *RAC1* abrogation require euthanization shortly after birth because of neurological problems, we used the same embryonic melanoblast reporter models to assess the downstream effects of P-Rex1 *in vivo* (Mackenzie *et al.*, 1997; Mort *et al.*, 2010; Li *et al.*, 2011). Melanocyte-specific reporter mouse strains employed were *Tyr::Cre Z/EG*, which drives green fluorescent protein expression in the melanoblast lineage, and *DCT::β-galactosidase* (otherwise referred to as *DCT-lacZ*).

First, we hypothesized that, if the effects of P-Rex1 were mediated exclusively via Rac1, double mutant *Tyr::Cre* $Rac1^{fl/fl}$; $P\text{-}Rex1^{-/-}$ mice would exhibit the same coat color phenotype as *Tyr::Cre* $Rac^{fl/fl}$ mice alone. However, *Tyr::Cre* $Rac^{fl/fl}$; $P\text{-}Rex1^{-/-}$ mice display a dramatic alteration in coat color phenotype from *Tyr::Cre* $Rac^{fl/fl}$ mice ($n=7$; Figure 1a). The ventral and dorsal coats of these mice are almost entirely white, with hypo-pigmented limbs and tail. Graying pigmented areas were only observed in the head coat. We concluded from this experiment that P-Rex1 and Rac1 together constitute fundamental signaling components of the mouse coat color phenotype, with minimal rescue of melanoblast development conferred by other GEFs or Rho-GTPases. It was also clear that P-Rex1 must be able to exert phenotypic effects other than via Rac1.

To explore the Rac1-independent effects of P-Rex1 further, we crossed *Tyr::Cre* $Rac^{fl/fl}$; $P\text{-}Rex1^{-/-}$ mice with mice carrying the melanoblast reporter *DCT-lacZ* transgene (methods detailed in Lindsay *et al.*, 2011). Relative to *Tyr::Cre* $Rac^{fl/fl}$ mice or $P\text{-}Rex1^{-/-}$ embryos alone, *Tyr::Cre* $Rac^{fl/fl}$; $P\text{-}Rex1^{-/-}$

Abbreviations: GEF, guanine-nucleotide exchange factor; OHT, 4-hydroxytamoxifen; PREX1, PIP_3-dependent Rac-exchanger 1

Accepted article preview online 30 July 2014; published online 11 September 2014

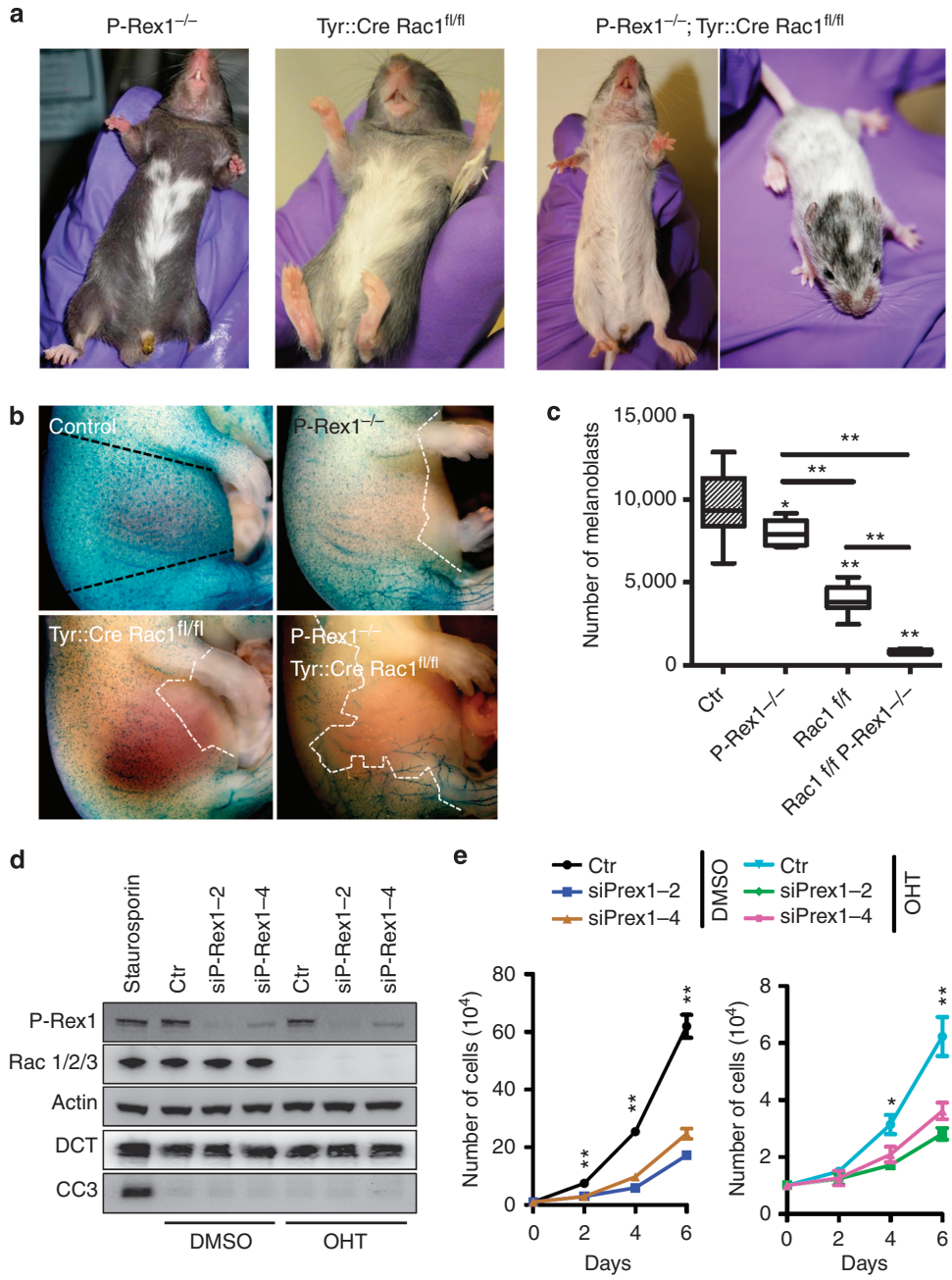

Figure 1. P-Rex1 and Rac1 are fundamental components of a mouse coat color phenotype. (**a**) Ventral coats of *P-Rex1*$^{-/-}$, *Tyr::Cre Rac1*$^{fl/fl}$ and *P-Rex1*$^{-/-}$; *Tyr::Cre Rac1*$^{fl/fl}$mice. Final photomicrograph shows dorsal and head coat of *Tyr::Cre Rac1*$^{fl/fl}$;*P-Rex1*$^{-/-}$ mice. All mice were bred from a pure genetic background (C57Bl6). A total of 7 *Tyr::Cre Rac1*$^{fl/fl}$;*P-Rex1*$^{-/-}$ mice were bred; as *Tyr::Cre Rac1*$^{fl/fl}$ mice have a limited life span and no breeding potential, *Tyr::Cre Rac1*$^{fl/+}$ mice were crossed with *P-Rex1*$^{-/-}$ mice to produce approximately one in four *Tyr::Cre Rac1*$^{fl/fl}$;*P-Rex1*$^{-/-}$ pups. (**b**) Representative photos of *DCT-lacZ* melanoblast distribution observed in *wild-type* (control), *P-Rex1*$^{-/-}$, *Tyr::Cre Rac1*$^{fl/fl}$, and *Tyr::Cre Rac1*$^{fl/fl}$;*P-Rex1*$^{-/-}$ embryos at E15.5. Black interrupted lines represent the area used for melanoblast quantification shown in **c**. White demarcated lines represent typical areas of melanoblast sparing visualized for each phenotype ($n=3$). (**c**) Number of melanoblasts in *wild-type* (Ctr), *P-Rex1*$^{-/-}$ ('P-Rex1 −/−'), *Tyr::Cre Rac1*$^{fl/fl}$ ('Rac1 f/f'), and *Tyr::Cre Rac1*$^{fl/fl}$;*P-Rex1*$^{-/-}$ ('Rac1 f/f P-rex1 −/−') embryos at E15.5 (≥ 5 embryos). Lower quartile, median, and upper quartile are shown. $^{**}P<0.01$ by *t*-test; $^{*}P<0.05$ by *t*-test. (**d**) Western blots of the primary melanocyte cell line, small interfering RNA (siRNA) treated as indicated, then treated with DMSO or 4-hydroxytamoxifen (OHT) for 5 days were probed with antibodies as indicated; Ctr, control siRNA–treated cells. (**e**) Growth curve of the primary melanocyte cell line, siRNA-treated as indicated, then treated with DMSO or OHT. Each point (mean ± SEM) is from three replicates of three independent experiments. Asterisks represent difference between control siRNA–treated cells and P-Rex1 siRNA–treated cells at the same time point; Ctr, control siRNA-treated cells.

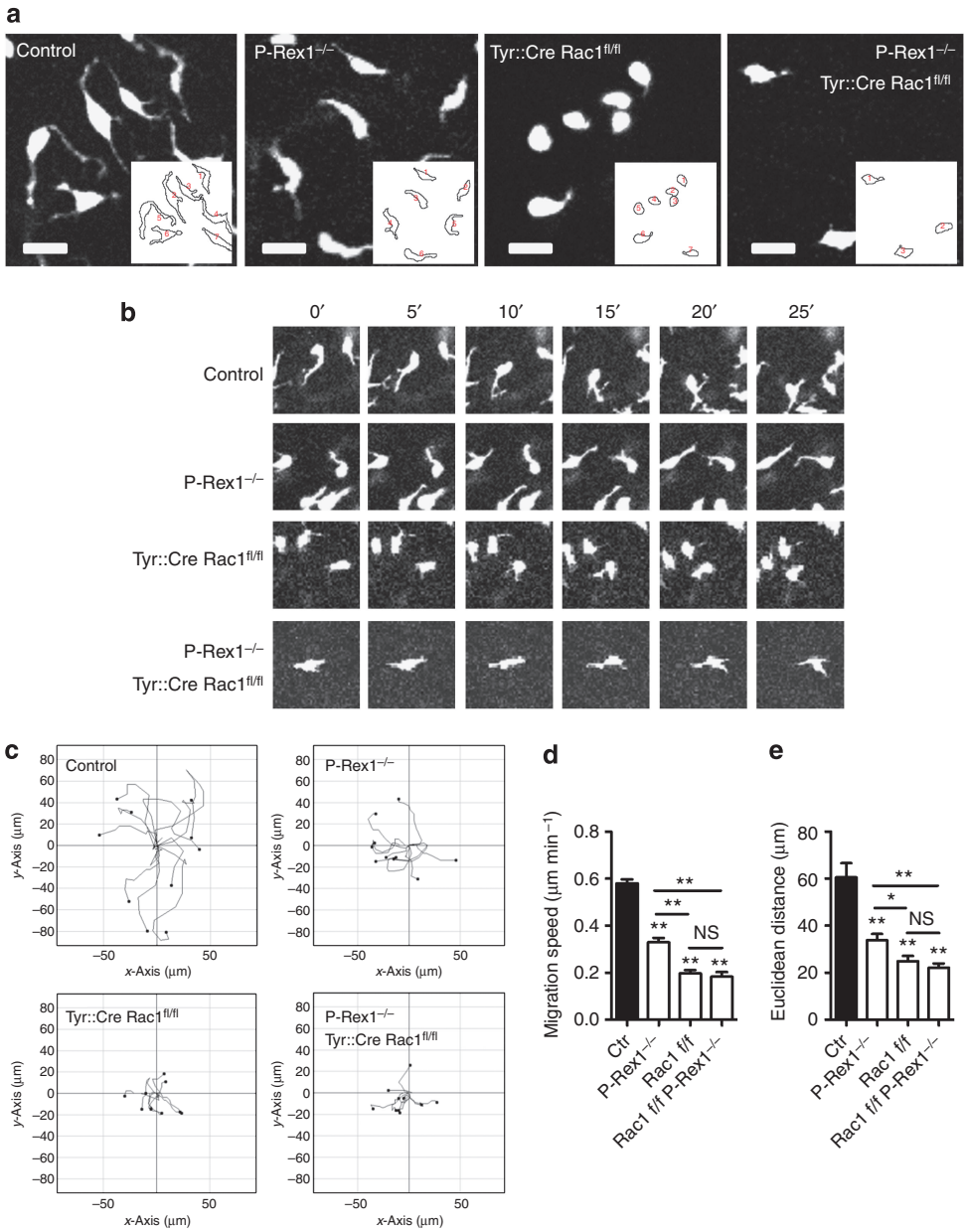

Figure 2. P-Rex1 has no additional effect on migration compared with Rac1 alone. All experiments show embryo skin explants at E15.5 (**a**) Combined Z-stack confocal images of Z/EG melanoblasts from *wild-type* (control), *P-Rex1*$^{-/-}$, *Tyr::Cre Rac1*$^{fl/fl}$, and *Tyr::Cre Rac1*$^{fl/fl}$*;P-Rex1*$^{-/-}$ embryos. Scale bars = 10 μm. (**b**) Representative photomicrographs showing live imaging of Z/EG melanoblasts in the skin of *wild-type*, *P-Rex1*$^{-/-}$, *Tyr::Cre Rac1*$^{fl/fl}$, and *Tyr::Cre Rac1*$^{fl/fl}$*; P-Rex1*$^{-/-}$ embryos at E15.5 ($n = 3$). Standard image measured at ×20 magnification was 635 × 635 μm. (**c**) Three-hour tracks of melanoblasts from the same genotypes. (**d**) Migration speed of Z/EG melanoblasts in *wild-type* (Ctr), *P-Rex1*$^{-/-}$ ('P-Rex1 −/−'), *Tyr::Cre Rac1*$^{fl/fl}$ ('Rac1 f/f'), and *Tyr::Cre Rac1*$^{fl/fl}$*;P-Rex1*$^{-/-}$ ('Rac1 f/f P-rex1 −/−') embryos (⩾5 embryos). $^{**}P < 0.01$ by *t*-test; $^{*}P < 0.05$ by *t*-test. (**e**) Z/EG melanoblast persistence, same genotypes, and annotation to that noted in **d**. Error bars indicate mean ± SEM. NS, nonsignificant.

embryos at E15.5 displayed a substantial reduction in melanoblast numbers across their entire body (Figure 1b and c). To assess whether the cause of this reduction in melanoblast numbers could be accounted for by decreased proliferation ± increased cell death, we next treated our previously described primary immortalized *Tyr::CrER2 INK4a*$^{-/-}$ *Rac*$^{fl/fl}$ melanocyte cell line with short interfering RNA to P-Rex1 (methods detailed in Li *et al.*, 2012). The use of this model system also allowed us to delete Rac1 function when these cells were treated with 4-hydroxytamoxifen (OHT). We first used western blotting to confirm that efficient P-Rex1 knockdown and OHT-induced Rac deletion were achieved (Figure 1d). There was no increase in cleaved caspase-3 evident in the absence of P-Rex1 and/or Rac, suggesting that the reduced cell numbers observed in *Tyr::Cre Rac*$^{fl/fl}$*; P-Rex1*$^{-/-}$ embryos were not accounted for by increased cell death (Figure 1d). Growth curves and anti-BrdU immunofluorescence of the same cell lines confirmed that there was

a reduced proliferation in P-Rex1-depleted cells, both in the presence and absence of OHT (Figure 1e; Supplementary Figure S1a and b online). Taken together, these results suggest, in addition to our previously reported effects of Rac1 deletion on mouse coat color, that the loss of a Rac1-independent proliferative effect of P-Rex1 also contributes to the coat color phenotype observed in *Tyr::Cre Rac$^{fl/fl}$; P-Rex1$^{-/-}$* mice (Li *et al.*, 2011).

In line with our previous characterization of the P-Rex1 knockout phenotype alone, we next decided to delineate whether the coat color phenotype of *Tyr::Cre Rac$^{fl/fl}$; P-Rex1$^{-/-}$* mice could also be a consequence of reduced melanoblast migration (Lindsay *et al.*, 2011). To assess this, mice with the *Z/EG* double reporter transgene were crossed with *Tyr::Cre Rac$^{fl/fl}$; P-Rex1$^{-/-}$* mice, driving green fluorescent protein expression in the melanoblast lineage (methods detailed in Lindsay *et al.*, 2011; Figure 2a). Live imaging of melanoblasts was performed using E15.5 embryo skin from each genotype (Figure 2b; Supplementary Movies S1–3 online). Consistent with our previous work, significant reductions in migration speed were observed between wild-type, *P-Rex1$^{-/-}$* and *Tyr::Cre Rac$^{fl/fl}$* melanoblasts (Figure 2c and d). However, there was no significant difference in speed between *Tyr::Cre Rac$^{fl/fl}$; P-Rex1$^{-/-}$* and *Tyr::Cre Rac$^{fl/fl}$* melanoblasts alone, suggesting that there was no change in migratory characteristics to account for the *Tyr::Cre Rac$^{fl/fl}$; P-Rex1$^{-/-}$* phenotype (Figure 2c and d). These results were matched by similar differences between the same genotypes when Euclidean distance was measured (Figure 2e), as well as no observable change in cell morphology evident in *Tyr::Cre Rac$^{fl/fl}$; P-Rex1$^{-/-}$* compared with *Tyr::Cre Rac$^{fl/fl}$* melanoblasts alone (Supplementary Figure S1c online; methods detailed in Helmy and Azim, 2012). Finally, no cell death was seen in our melanoblast time-lapse movies of any genotype, again suggesting that P-Rex1 contributes to coat color phenotype by promoting cell proliferation using a Rac1-independent mechanism (Li *et al.*, 2011; Supplementary Movies S1–3 online; methods detailed in Lindsay *et al.*, 2011).

To conclude, we have elucidated a proliferative role of P-Rex1 when Rac1 is deleted. As E15.5 migratory characteristics are not altered in the *Tyr::Cre Rac$^{fl/fl}$; P-Rex1$^{-/-}$* double mutant embryos, this suggests that the role of P-Rex1 in migration is almost exclusively mediated via Rac1. Here we focused on E15.5 embryos, a useful time point to observe the late migratory effects observed with previously described Prex and Rac phenotypes (Li *et al.*, 2011; Lindsay *et al.*, 2011). With a greater number of embryos, we would have performed further embryo time-point analyses at E13.5 to ensure there was no earlier melanoblast migratory deficit that could contribute to this phenotype, although even this experiment could not completely exclude such a possibility.

One potential Rho-GTPase, RhoG, is a likely candidate for P-Rex1 interaction: it is the most structurally similar Rho-GTPase to Rac and has been shown to cooperate with Rac for induction of cell transformation (Roux *et al.*, 1997). Moreover, there are distinct regulatory and functional similarities between P-Rex1 and Vav proteins, which have been characterized as the predominant GEFs required for RhoG activation (Samson *et al.*, 2010; Lawson *et al.*, 2011). Further studies are underway to investigate the phenotypes of these and other potential Rho-GTPases in melanoblast migration and melanomagenesis. Given that there is now considerable effort to generate Rac1 inhibitors, our data would suggest functions for proteins upstream of Rac1 that may become further therapeutic targets in melanoma. All experiments were conducted and approved in accordance with institutional and UK guidelines, and all animal studies were performed in accordance with local regulatory guidelines.

CONFLICT OF INTEREST

The authors state no conflict of interest.

ACKNOWLEDGMENTS

This research was supported by a Medical Research Council clinical fellowship (CRL), CRUK, and a European Research Council consolidator grant (OJS). We thank Colin Nixon and Margaret O'Prey, as well as the biological services, histology, and imaging staff at the CRUK Beatson Institute for Cancer Research in general. We also thank Catherine Winchester for her assistance with checking the manuscript.

Colin R. Lindsay[1], Ang Li[1], William Faller[1], Brad Ozanne[1], Heidi Welch[2], Laura M. Machesky[1] and Owen J. Sansom[1]

[1]Cancer Research UK Beatson Institute, Glasgow, UK and [2]The Babraham Institute, Cambridge, UK
E-mail: o.sansom@beatson.gla.ac.uk

SUPPLEMENTARY MATERIAL

Supplementary material is linked to the online version of the paper at http://www.nature.com/jid

REFERENCES

Barber M, Donald S, Thelen S *et al.* (2007) Membrane translocation of P-Rex1 is mediated by G protein betagamma subunits and phosphoinositide 3-kinase. *J Biol Chem* 282: 29967–76

Berger MF, Hodis E, Heffernan TP *et al.* (2012) Melanoma genome sequencing reveals frequent PREX2 mutations. *Nature* 485:502–6

Helmy IM, Azim AMA (2012) Efficacy of ImageJ in the assessment of apoptosis. *Diagn Pathol* 7:15

Hill K, Krugmann S, Andrews DR *et al.* (2005) Regulation of P-Rex1 by phosphatidylinositol (3,4,5)-trisphosphate and Gbetagamma subunits. *J Biol Chem* 280:4166–73

Lawson CD, Donald S, Anderson KE *et al.* (2011) P-Rex1 and Vav1 cooperate in the regulation of formyl-methionyl-leucyl-phenylalanine-dependent neutrophil responses. *J Immunol* 186:1467–76

Li A, Ma Y, Yu X *et al.* (2011) Rac1 drives melanoblast organization during mouse development by orchestrating pseudopod-driven motility and cell-cycle progression. *Dev Cell* 21:722–34

Li A, Ma Y, Jin M *et al.* (2012) Activated mutant NRas(Q61K) drives aberrant melanocyte signaling, survival, and invasiveness via a Rac1-dependent mechanism. *J Invest Dermatol* 132:2610–21

Lindsay CR, Lawn S, Campbell AD *et al.* (2011) P-Rex1 is required for efficient melanoblast migration and melanoma metastasis. *Nat Commun* 2:555

Mackenzie MA, Jordan SA, Budd PS *et al.* (1997) Activation of the receptor tyrosine kinase Kit is required for the proliferation of melanoblasts in the mouse embryo. *Dev Biol* 192: 99–107

Mort RL, Hay L, Jackson IJ (2010) *Ex vivo* live imaging of melanoblast migration in embryonic mouse skin. *Pigment Cell Melanoma Res* 23:299–301

Roux P, Gauthier-Rouvière C, Doucet-Brutin S *et al.* (1997) The small GTPases Cdc42Hs, Rac1 and RhoG delineate Raf-independent

pathways that cooperate to transform NIH3T3 cells. *Curr Biol* 7:629–37

Samson T, Welch C, Monaghan-Benson E *et al.* (2010) Endogenous RhoG is rapidly activated after epidermal growth factor stimulation through multiple guanine-nucleotide exchange factors. *Mol Biol Cell* 21:1629–42

Sugihara K, Nakatsuji N, Nakamura K *et al.* (1998) Rac1 is required for the formation of three germ layers during gastrulation. *Oncogene* 17:3427–33

Welch HC, Coadwell WJ, Ellson CD *et al.* (2002) P-Rex1, a PtdIns(3,4,5)P3- and Gbetagamma-regulated guanine-nucleotide exchange factor for Rac. *Cell* 108:809–21

Rationale for the Development of Speckled Hyperpigmentation in the Areas of Psoriatic Plaques after Treatment with Biologic Agents

Journal of Investigative Dermatology (2015) **135,** 318–320; doi:10.1038/jid.2014.297; published online 21 August 2014

TO THE EDITOR

We read with great interest the original article by Wang *et al.* (2013) published in this journal.

The authors investigated the effects of proinflammatory cytokines (i.e., TNF and IL-17) on epidermal melanocytes and their contribution to postinflammatory hyperpigmentation in psoriatic patients.

They demonstrated that primary human melanocytes respond to IL-17 and/or TNF stimulation forming clusters and modulating the expression of a broad panel of genes. In particular, synergistic stimulation of melanocytes with IL-17 and TNF leads to increased expression of mitogenic cytokines and growth factor genes (e.g., *CXCL-1 and IL-8*) and downregulates the pigmentation signaling pathway and melanin production (e.g., *c-Kit, MC1R, Mitf, Dct*). There is also a significant decrease of tyrosinase levels and cellular melanin content.

Moreover, given the pathogenic role of TNF and IL-17 in psoriasis, Wang *et al.* investigated the pigmentation genes in psoriatic plaques and, as expected, they found a broad inhibition of genes involved in melanin synthesis, catalytic enzymes, and lineage-specific melanocyte transcriptional factors. Indeed, they found overexpression of a MC1R keratinocyte–derived antagonist (i.e., beta defensin 3) in psoriatic plaques.

Taken together, all these findings suggest that the psoriatic inflammatory milieu exerts a protective role against melanogenesis. Recently, we (Di Cesare *et al.*, 2013) and others (Balato *et al.*, 2011) reported that psoriatic patients have a low number of melanocytic nevi as compared with healthy controls. Indeed, we found that the probability of having melanocytic nevi in psoriatic patients was 82% lower compared with controls even independently of personal and medical confounders such as sociodemographic factors, skin type and acute and/or chronic sun exposure, family history of cancer, and psoriasis-associated factors, such as disease family history, obesity, metabolic syndrome, cigarette smoking, and alcohol consumption (Di Cesare *et al.*, 2013).

In their paper, Wang *et al.* (2013) also demonstrated that psoriatic skin has an increased number of melanocytes, with a positive MelanA staining. They reported that psoriatic lesional skin, and not nonlesional or healthy control skin, is Ki67 + /MART-1 + . This means that, despite IL-17/TNF brake on melanogenesis, melanocytes do not migrate from the inflamed skin to IL-17/TNF-free areas, but conversely they still infiltrate the plaques, expressing CCL20 and other adhesion molecules (Wang *et al.*, 2013). Therapeutic neutralization of IL-17 and TNF with biologic agents is able to recover pigmentation signaling, leading to postinflammatory hyperpigmentation in the areas corresponding to the plaques that were enriched with melanocytes. In our opinion, this is a clue point to elucidate the mechanism of posttherapeutic development of lentigines confined to the areas of preexisting psoriatic plaques that has been reported following phototherapy, topical treatments, or biologic agents (Burrows *et al.*, 1994; Ana Costa *et al.*, 2009; Santos-Juanes *et al.*, 2008; Martì *et al.*, 2009; Bardazzi *et al.*, 2012).

We observed the appearance of speckled hyperpigmentation within the psoriatic plaque areas during treatment with biologics in six patients (2 F, 4 M; median age: 64 years; range: 50–75 years) during the treatment with adalimumab (3/6) (Figure 1), infliximab (1/6), ustekinumab (1/6), and etanercept (1/6) (Figure 2). A written consent for skin biopsies and photographic documentation was obtained for each patient. All patients were affected with moderate-to-severe psoriasis (psoriasis area and severity index > 10) and 5/6 had concomitant psoriatic arthritis; 4/6 patients had < 10 nevi, and 2/6 had a total number of nevi between 10 and 30. All patients had received several cycles of topical (corticosteroids and/or vitamin D analogue, retinoids) and systemic treatments including ciclosporin (5/6), methotrexate (3/6),

Abbreviation: TNF, tumor necrosis factor

Accepted article preview online 18 July 2014; published online 21 August 2014